ARCHIVES OF METALLURGY

Volume 45 2000 Issue 3

JAN DUTKIEWICZ*, TOMASZ CZEPPE*,
JAN MORGIEL*, WOJCIECH MAZIARZ*

PROPERTIES AND STRUCTURE OF THE SHAPE-MEMORY MELT SPUN CuAlNiMnTi(Zr) RIBBONS

WŁASNOŚCI I STRUKTURA TAŚM CuAlNiMnTi(Zr) KRYSTALIZOWANYCH Z FAZY CIEKŁEJ WYKAZUJĄCYCH PAMIĘĆ KSZTAŁTU

The CuAlNiMnTi(Zr) alloys with 0 – 5% Mn and up to 1% Ti or Zr (in wt.%) were cast using melt spinning method at linear wheel rate 3.5 – 31 m/s. Fine grain ribbons with good shape memory effect within 0 – 200°C were obtained without an additional heat treatment. The microstructure was analyzed using optical, scanning and transmission electron microscopy, while their mechanical properties were examined in tensile test using Instron TT-DM machine. The martensite transformation in ribbons was found to be depressed to lower temperatures with decreasing grain size accordingly to the equation $\Delta M = k \cdot d^{-1/2}$. The addition of grain refiners like Ti or Zr decreased grain size even to sub micron range. At the highest of applied linear wheel rate of 30.6 m/s a dissolution of Ti within β matrix was observed, while at lower rates the cubic Cu_2TiAl type precipitates were formed. The ribbons containing CuAlNi 2wt.%Mn0.4wt.%Ti showed best mechanical properties.

Stopy CuAlNiMnTi(Zr) zawierające do 5% Mn i 1% Ti lub Zr (% wag.) zostały odlane na miedziany walec wirujący przy szybkości liniowej od 3,5 do 31 m/s, co pozwoliło uzyskać drobnoziarniste taśmy wykazujące pamięć kształtu w zakresie od 0 do 200°C. Mikrostrukturę analizowano w mikroskopach optycznym, skaningowym i transmisyjnym, a własności mechaniczne oceniano w próbie rozciągania na maszynie Instron. Temperatura przemiany martenzytycznej w taśmach obniżała się wraz ze zmniejszeniem wielkości ziarna zgodnie z zależnością $\Delta M = k \cdot d^{-1/2}$. Dodatek Ti lub Zr pozwolił uzyskać nawet submikronowe ziarno. Przy najwyższej z zastosowanych prędkości liniowej walca, tj. 30,6 m/s stwierdzono rozpuszczanie Ti w fazie β, podczas gdy przy odlewaniu z niższymi prędkościami dochodziło do tworzenia wydzieleń typu Cu_2TiAl. Najlepsze własności mechaniczne wykazywały taśmy CuAlNi 2%wag.Mn0,4%wag.Ti.

* INSTYTUT METALURGII I INŻYNIERII MATERIAŁOWEJ IM. A. KRUPKOWSKIEGO PAN, 30-059 KRAKÓW, UL. REYMONTA 25

1. Introduction

Copper based shape memory melt spun ribbons have been intensively studied in recent years because of their fine grain size [1 – 7] and superior mechanical properties [7, 8] as compared with the bulk. Thin ribbons possessing the β structure are obtained in one step allowing to overcome a complicated thermo-mechanical processing of the bulk material, which is usually brittle and therefore difficult to handle.

A decrease of martesite transformation temperature in ribbons connected with finer grain size obtained in this process [3, 5, 8] against that of bulk material is a typical feature of the rapidly quenched CuAlX (X = Ni, Zn, Mn) alloys. However, in the CuAlNiMnTi (CANTIM) alloy an increased content of titanium in the β phase metastable solid solution is additionally lowering the characteristic temperatures of martensite transformation. Due to complexity of microstructure of rapidly quenched ribbons the role of various factors on martensite transformation is still not well understood.

The aim of the present paper was to analyze the effect of melt spinning conditions on mictrostructure and characteristic martensitic temperatures in CuAlNi, CuAlNiTi and CuAlNiMnTi ribbons.

2. Experimental procedure

Alloys of composition presented in table 1 were cast using a Balzers high frequency furnace under the protective argon atmosphere. The alloys composition was chosen such that it would show the reverse martensitic transformation between

TABLE 1

Chemical composition of the investigated alloys (in wt.%)

Alloys	Cu	Al	Ni	Mn	Ti	Zr	Ms [°C] bulk
89	bal.	13.0	4.0	----	----	----	183
90	bal.	11.8	4.0	3.0	----	----	103
90 B	bal.	11.5	4.0	3.0	----	----	153
91	bal.	13.5	3.2	----	1.0	---	67
91 B	bal.	13.0	3.2	----	1.0	----	170
91 C	bal.	13.0	3.2	----	----	1.0	176
92	bal.	11.9	5.0	2.0	1.0	----	161
92 C	bal.	11.9	5.0	2.0	----	1.0	99
94	bal.	11.4	2.5	5.0	0.4	----	77
95	bal.	11.8	5.0	2.0	0.4	----	140
96	bal.	10.7	2.3	4.8	0.4	----	147
98	bal.	10.9	2.1	5.0	0.4	----	110
99	bal.	12.0	5.0	2.0	0.5	---	126

100°C and 150°C. Thin ribbons were cast using specially constructed apparatus on the rotating copper wheel of diameter 100 mm placed within the box filled with helium. Pieces of alloys (2–3 cm^3) were melted using high frequency generator. The alloys were ejected from the quartz tube of diameter 20 mm with a bottom round hole $\phi = 0.7$ mm on the rotating copper drum under 0.14 MPa pressure of helium on the wheel rotating at the linear speed between 3.5–31 m/sec.

The ribbons were characterized using a DuPont 910 differential scanning calorimeter, Philips CM20 transmission electron microscope and Philips XL 30 scanning microscope. Thin foils were electropolished in a double jet Fishione apparatus using H_3PO_4/CrO_3 electrolyte. The ribbons were tested using an Instron tensile machine.

3. Results

3.1. Description of ribbons

Optical microstructures presenting grain size of bulk alloys with various alloying additions are shown in Fig. 1. Average results concerning the characteristic size and quality of ribbons are presented in table 2. The estimation of ribbons porosity and surface roughness determined their quality. Thickness and width of the

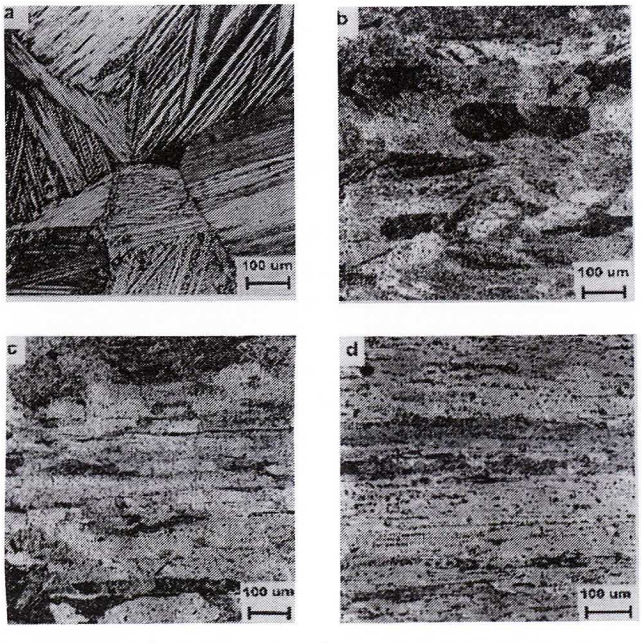

Fig. 1. Optical mictrostructures of rolled, homogenized and quanched bulk alloys: (a) 90, (b) 94, (c) 95, and (d) 92

ribbons cast with rates from 16 to 30.6 m/s was similar, while lower rates produced thicker and wider ribbons. Porosity happens at the highest of the applied rates, while twisted and deformed ribbons may result under the lowest of applied rate.

TABLE 2

Parameters of CuAlNiMn and CuAlNiMnTi ribbons cast at different wheel speeds

Voltage [V]	Rate [m/s]	Thickness [mm]	Width [mm]	Quality
50	30.6	0.07	2.1	poor
45	26.4	0.07	2.2	v. good
40	22.2	0.07	2.8	v. good
35	16.0	0.07	2.5	v. good
30	8.5	0.12	3.7	v. good
25	3.3	0.40	4.9	good

3.2. DSC measurements of characteristic martensite transformation temperatures

The calorimetric curves of bulk CuAlNi and CuAlNiMn alloys present well defined thermal effects connected with the martensitic and reverse phase transformation with a maximum heat of transformation up to 10 J/g for the bulk alloys (Fig. 2). Measurements of enthalpy of ribbons gave much smaller effects of about 7 J/g. The peak start (M_s) and peak maximum (M_p) temperatures are shifted to the lower range with the increasing wheel speed.

The CuAlNiMnTi ribbons cast at medium wheel speed frequently show peaks splitting both on cooling and heating curves as presented in Fig. 3. The highest of applied wheel speeds results in very wide effects with enthalpy of transformation down to 3 J/g. Similarly, the CuAlNiZr ribbons are characterized by wider and slightly irregular peaks. The energy of the martensitic transformation in bulk alloy was about 10 J/g and lowered in the case of the ribbons to 8 J/g.

The DSC curves measured during forward and reverse martensite transformation in CuAlNiMn alloy shows single peaks for each effect, while similar curves for CuAlNiMnTi alloy presents peak splitting due to two or even three effects. Usually A_s and M_s temperatures are determined by tangent line to the peak side but for peaks with side maximum the values obtained with this method can not be easily compared with other data. Specially, neither the $(M_s+M_f)/2$ is not necessary equal to M_p nor $(A_s+A_f)/2$ does not denote A_p. Therefore, M_p and A_p were determined separately and presented together with respective M_s and M_f in Fig. 4. The lowering of the peaks

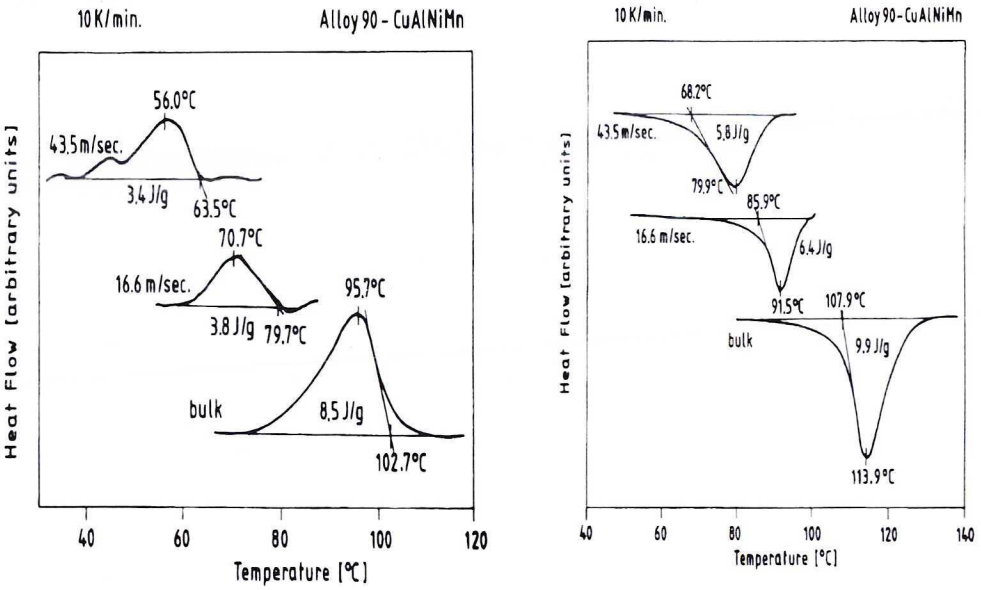

Fig. 2. DSC cooling (a) and heating (b) curves for CuAlNiMn (90) bulk and ribbons cast at various wheel speeds

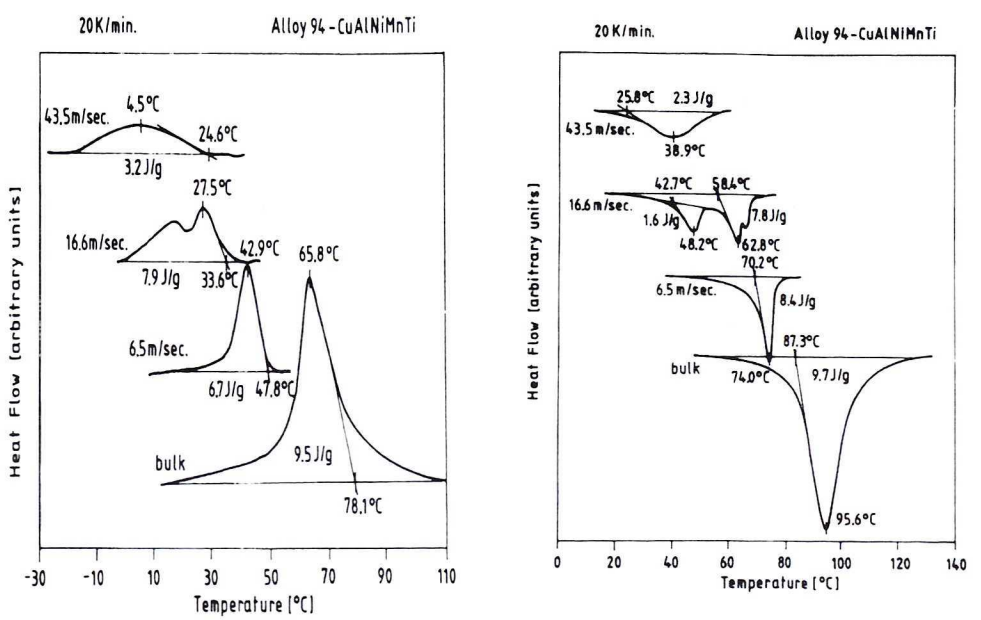

Fig. 3. DSC cooling (a) and heating (b) curves for CuAlNiMnTi (94) bulk and ribbons cast at various wheel speeds

height and formation of long tails at increasing wheel speed presents special problem in determination of the peak area and usually results in lack of precision in estimation of the transformation energy. The strong decrease of the characteristic temperatures at low wheel speed and their stabilization for higher ones is similar for both alloys. It indicates that the same mechanism is responsible for their control independently of their different bulk M_s temperatures. The CuAlNiZr ribbons showed similar changes but the final shift of martensite transformation in reference to the bulk alloy of the same composition is noticeably smaller (Fig. 5). The effect was caused by refinement of

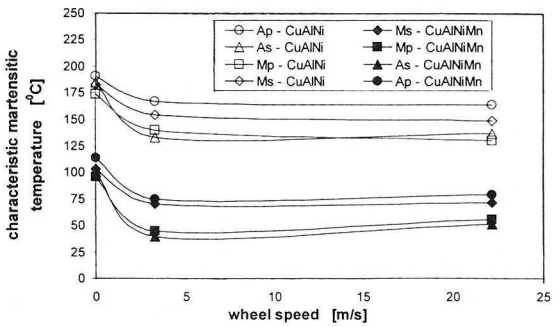

Fig. 4. Characteristic temperatures of CuAlNi and CuAlNiMn alloys cast at different wheel speed

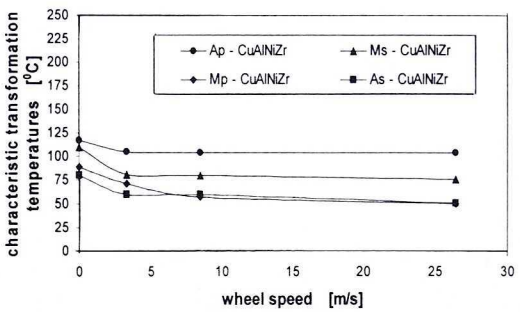

Fig. 5. Characteristic temperatures of CuAlNiZr alloys cast with different wheel speed

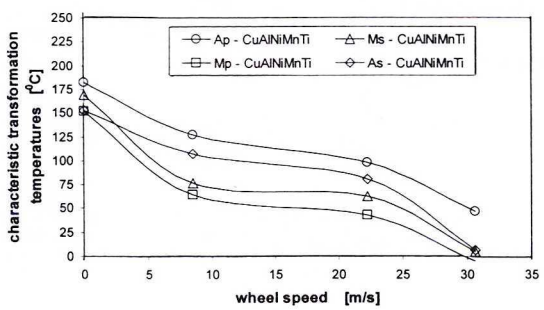

Fig. 6. Characteristic temperatures of CuAlNiTi alloys cast with different wheel speed

grain in bulk alloy caused by zirconium, so the difference between the grains size in bulk and ribbons were much smaller than for the other alloys.

The martensitic transformation in the CuAlNiMnTi ribbons is also shifted down in relation to their bulk alloy as shown in Fig. 6. However, the lowering of characteristic temperatures takes place for all investigated wheel speeds, while in all previously discussed alloys higher speeds do not bettered low ones.

3.3. TEM observations of structure of bulk alloys and ribbons

In order to correlate the observed shifts of the characteristic transformation temperatures in ribbons cast at different wheel speeds with the changes of microstructure, a transmission electron microscopy was applied. Fig. 7a shows the

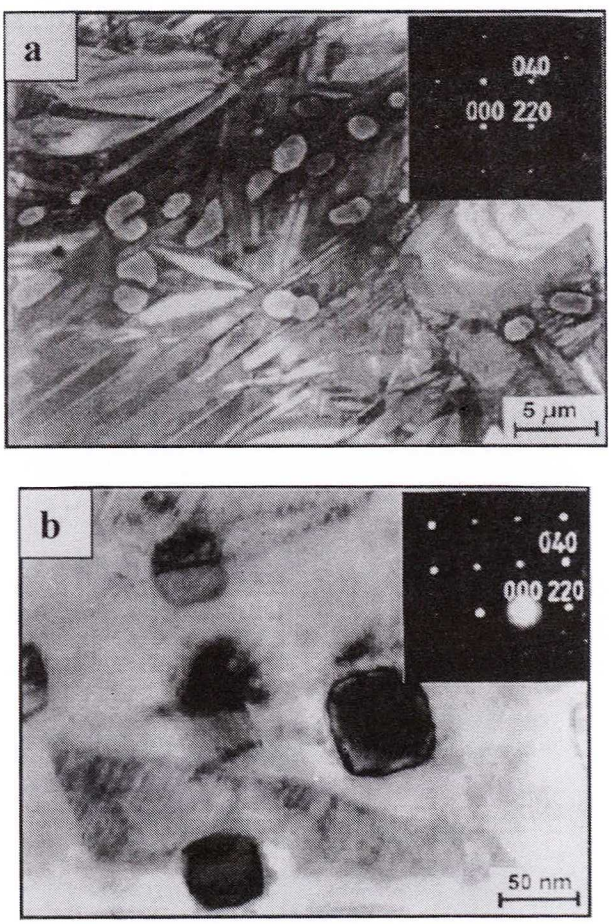

Fig. 7. Microstructure of a) bulk alloy 92 and b) ribbon 92 cast at 16.6 m/s with corresponding SADP from the precipitates as an inserts

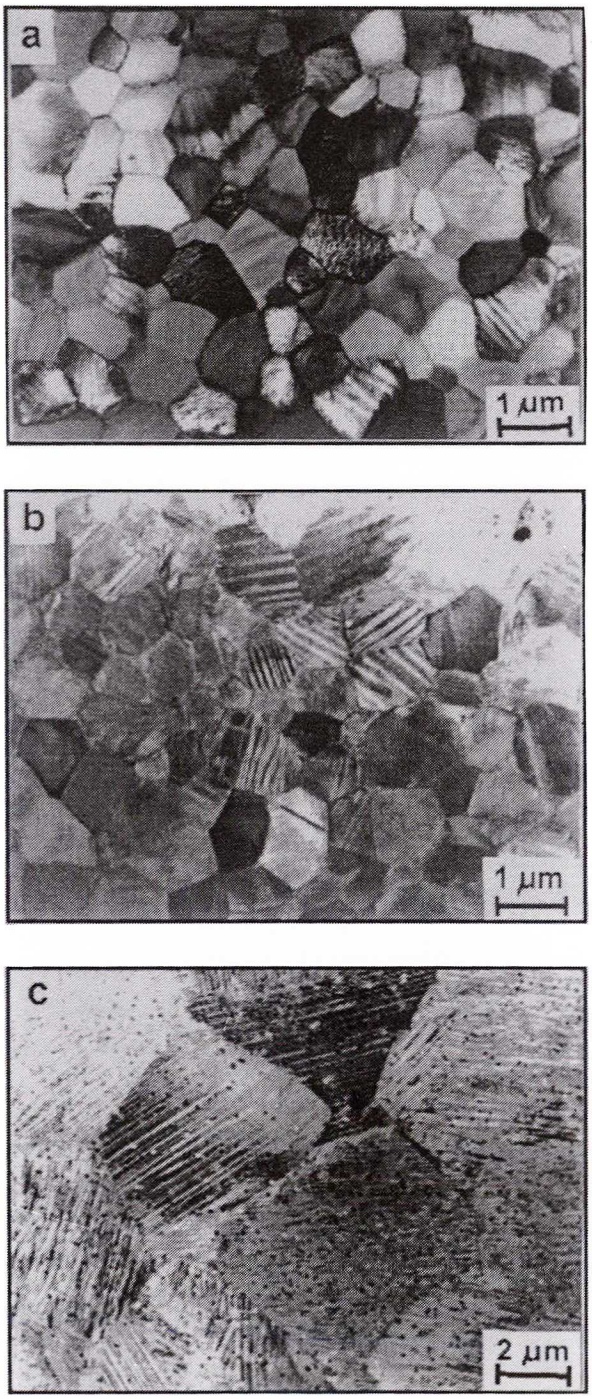

Fig. 8. Microstructure of ribbons of alloy 94 melt spun at various wheel speeds: (a) 22.2 m/s, b) 10.5 m/s and (c) 8.5 m/s

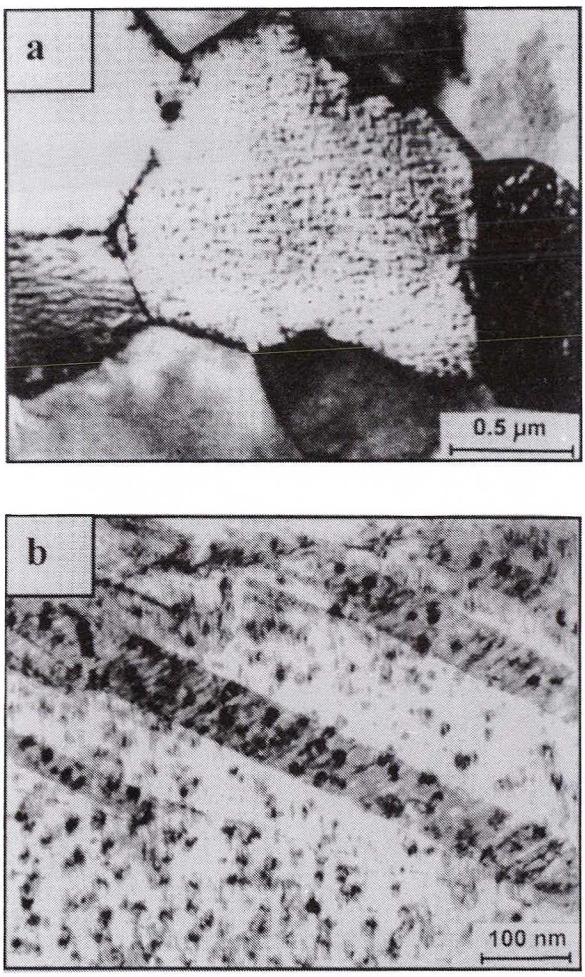

Fig. 9. Microstructure of ribbons cast at an of rate 22.2 m/s from alloys: a) Cu11.4Al2.5Ni5 Mn0.4Ti (94), b) Cu11.8Al5Ni2Mn0.4Ti (95)

martensite matrix with some large oval precipitates. The selected area diffraction pattern (SADP) from precipitates, shown as an insert in the right upper corner, gave a good match with the [100] orientation of the Cu_2AlTi phase. Analysis performed using an EDS system indicated relatively large content of nickel (up to 16 at.%) substituting copper in the compound. Fig. 7 b shows very small precipitates of square shape surrounded by thin martensite platelets in the ribbon of alloy 92 (cast at linear wheel speed of 16.6 m/s). The SADP taken from the small precipitate — placed as an insert — shows the Cu_2AlTi type phase identical as in the case of the bulk alloy. This indicates that the melt spinning does not affect the type of precipitates but causes only grain and precipitate size refinement.

Fig. 8. shows the series of microstructures of alloy 94 cast at various wheel speeds leading to different grain sizes. The ribbons (cast at rates between 3.3 m/s — 10.5 m/s) show martensitic platelets with fine Cu_2AlTi precipitates within grains of decreasing size from 8 to 0.5 μm respectively. The precipitates uniformly fill up all grains. The ribbon cast at 22.2 m/s shows the β phase grains

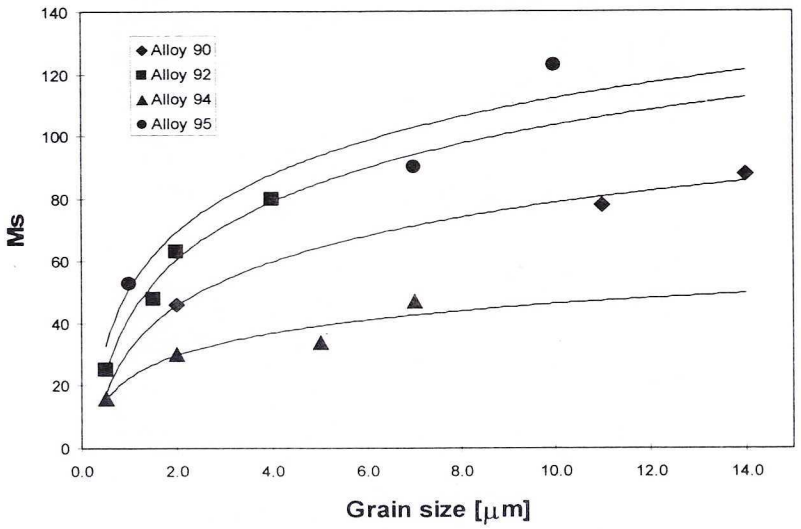

Fig. 10. Relationship of martensite start temperature M_s *vs.* grain size d

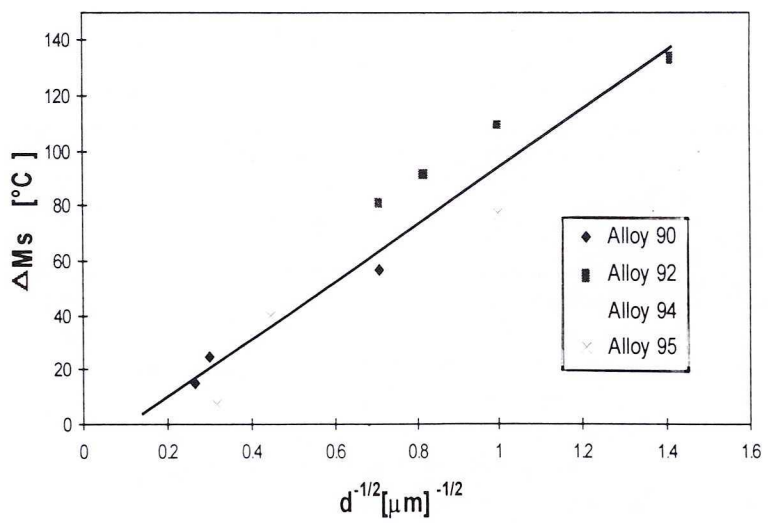

Fig. 11. Relationship of martensite start temperature M_s *vs.* grain size *vs.* $d^{-1/2}$

as the martensite transformation was shifted below room temperature at which the observations were performed. The microstructure of this alloy is better visible in the next microstructure (Fig. 9a) taken at the higher magnification. Within the β grains a modulated microstructure may be distinguished, which was most probably caused by the premartensitic surface effects [9]. However, decreasing manganese and simultaneous increasing nickel content causes that small precipitates like in Fig. 9b visible again even at highest wheel speed.

Fig. 10 shows the M_s *vs.* grain size relationship for the investigated CuAlNiMnTi ribbons melt spun at different cooling rates. One can see that with a decreasing grain size from 14 to about 4 μm the M_s temperature is only slightly lowered, but the decrease of the transformation temperatures is more rapid in the finer grain size range. Since much smaller grain size can be obtained for ribbons with titanium addition, they show the strongest changes in the characteristic temperatures. This effect is even better visible in the Fig. 11, where the same data are presented in the form of $\Delta M_s = f(d)^{-1/2}$ (where ΔM_s is equal to the difference between the M_s of the ribbon and of the bulk alloy and d is the grain size. Their relationship can be fitted as a straight line for all investigated alloys. It suggests that the effect of supersaturation of titanium is rather weak compared with the grain size effect. However, since there is a scatter of the data, one cannot exclude the influence of other factors, like atomic ordering, as suggested for the melt spun CANTIM alloys [6] and strains caused by precipitation [10].

3.4. Mechanical properties of ribbons

Fig. 12 presents $\sigma = f(\varepsilon)$ curves of ribbons tested at room temperature in the martensitic state. One can see that the ribbons prepared with higher quenching rate and therefore having smaller grain size exhibit always lower hardening. The ribbons of CuAlNiMnTi alloy show larger differences in hardening than those cast from the CuAlNiMn alloy. However, in both cases the strength of ribbons with smaller grain size was higher. The highest elongation was obtained in the case of ribbon 99 with 0.5 wt.%Ti, being even higher than that of ribbon 89, with much larger grains. Fig. 13 presents $\sigma = f(\varepsilon)$ curves for the same ribbons but tested at higher temperature, i.e. above A_f temperature, in the β phase. In such a case difference between ribbons with different grain sizes are not so large but ribbon 99 quenched with a higher rate exhibited again very high elongation.

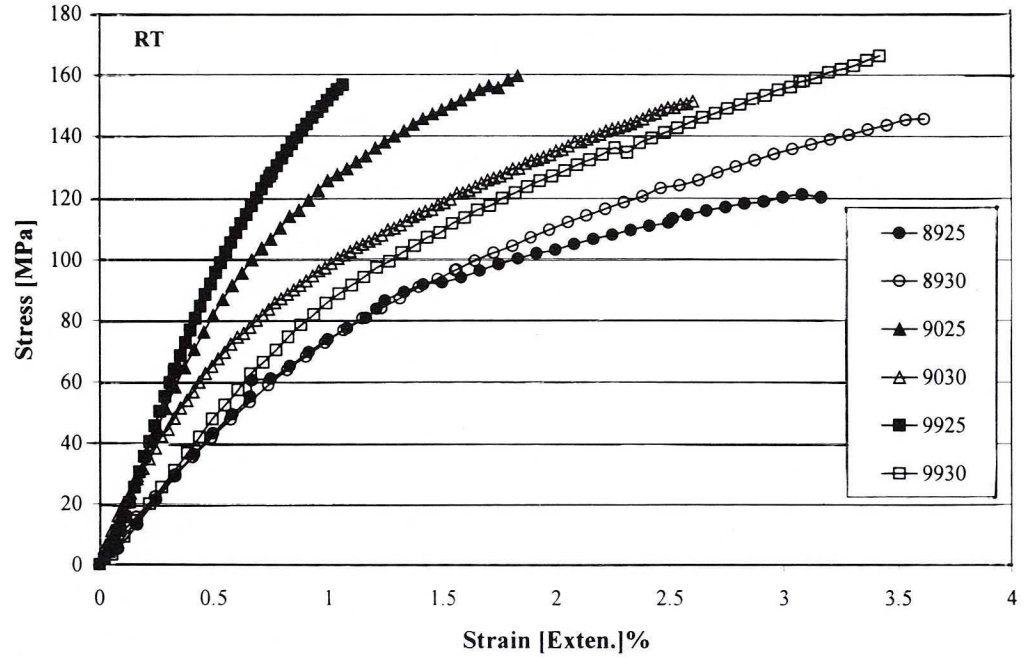

Fig. 12. Relation $\sigma = f(\varepsilon)$ for CuAlNi 89, CuAlNiMn 90 and CuAlMnTi 99 ribbons cast at 3.3 m/s (25) and 8.5 m/s (30) (deformation at R.T. in martensite phase)

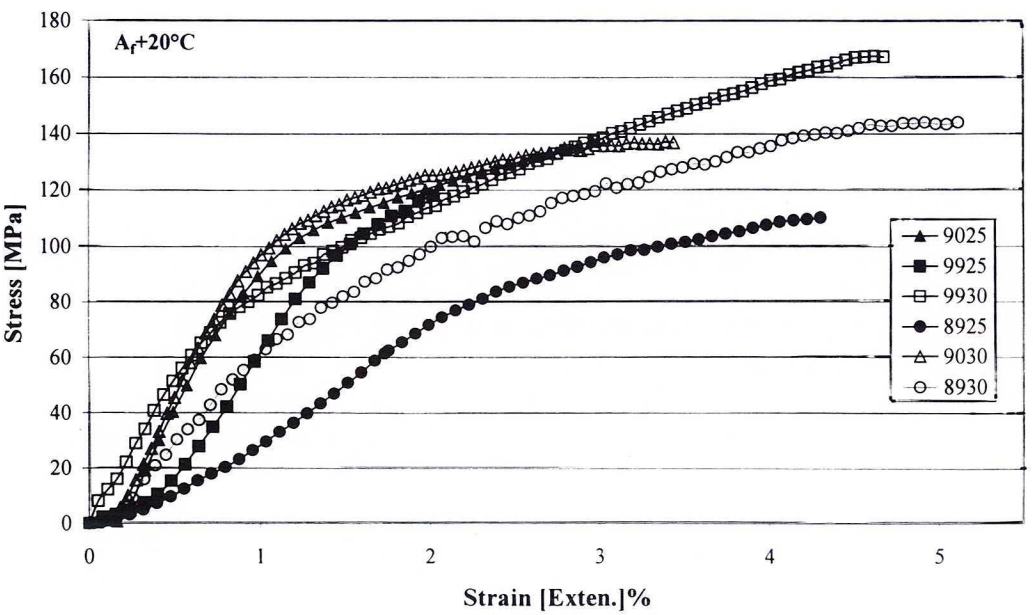

Fig. 13. Relation of $\sigma - \varepsilon$ for CuAlNi 89, CuAlNiMn 90 and CuAlNiMnTi 99 ribbons cast at 3.3 m/s (25) and 8.5 m/s (30) (deformation in β phase at $A_f + 20°C$ respectively)

4. Summary and conclusions

The investigation of several copper based alloys with different Al, Mn, Ni and Ti content proved that the melt-spining technique allows produce ribbons showing good shape memory effect without additional heat treatment. Their microstructure is characterized by a fine grain size even at a low wheel speed. Additions of classical grain refiners like titanium or zirconium to copper based alloys allow decrease the grain size to sub-micron range. The grain size was found to be the most effective factor in decreasing the martensite transformation range. The following conclusions were also drawn:

1. The alloy composition optimal for both good mechanical properties and high temperature transformation range was found to be that of Cu—12 wt.%Al—5 wt.% Ni—2 wt.%Mn—0.5 wt.%Ti.

2. Increase of cooling rate causes a rapid decrease of the size of Cu_2TiAl and Cu_2ZrAl precipitates in the CuAlNiMnTi and CuAlNiZr melt spun ribbons respectively. At highest cooling rate of 22 m/s dissolution of 0.5 wt.% titanium in the β phase of the alloy with the high manganese addition occurs.

3. High solidification rate i.e. fast wheel rotation, causes significant decrease of grain size within ribbons. The ribbons containing Ti and Zr may achieve much smaller sub-micron grain size than alloys without these additions. Transformation temperatures in all investigated ribbons fit the relationship $\Delta M_s = k \cdot d^{-1/2}$.

4. The structure of precipitates in the bulk and melt spun CuAlNiMnTi alloys were determined as cubic Cu_2TiAl type. They contain several percent of nickel substituting copper in this compound.

5. The CuAlNiZr alloy quenched at the wheel rate below 20 m/s shows large Cu_2AlZr precipitates at grain boundaries containing 11–13% of Ni. The increasing cooling rate up to 31 m/sec causes refinement of precipitates down to 20 nm. They are coherent with the matrix, which is one of the reasons for widening of the transformation hysteresis.

6. The tensile tests showed highest elongation in the case of the ribbons with 2 wt. % manganese and 0.4% wt.% of Ti addition. These alloys also showed the best yield strength and ultimate tensile strength due to the smallest grain and precipitate size.

Acknowledgement

The financial support by INCO – COPERNICUS project no: IC15960704 is gratefully acknowledged.

Keynote paper presented at the Deformation-Induced Mictrostructures and Properties of Metallic Materials, in frame of the *IVth International Conference on Non-Ferrous Metals and Alloys'99*, June 24–25, 1999, on occasion of the 80th anniversary of the University of Mining and Metallurgy, Cracow, Poland.

REFERENCES

[1] G. Scarsbrook, W. M. Stobbs, Acta Metall **35,** 47 (1987).
[2] S. Eucken, E. Hornbogen, Proc. ICOMAT-86, J I M, 780 Sendai 1987.
[3] S. S. Leu, Y. C. Chen, R. D. Jean, J. Materials Sci. **27,** 2792 (1992).
[4] A. Ahmed, S. W. Husain, Z. Iqbal, F. H. Hashmi, A. Q. Khan, Scripta Met. **22,** 803 (1988).
[5] J. Dutkiewicz, J. Morgiel, T. Czeppe, E. Cesari, ESOMAT 97, J. Phys IV (1997) Coll. C5-167.
[6] J. H. Zhou, D. P. Dunne, G. W. Dillamore, N. F. Kennon, Proc. ICOMAT-92 Monterey Institute for Advanced Studies, 1083 Monterey 1992.
[7] S. Matsuoka, M. Hasebe, R. Oshima, F. E. Fujita, Jpn. J. Appl. Phys., Lett. **22(8)** L528 (1983).
[8] S. Eucken, E. Hornbogen, Proc. ICSMA 7, Pergamon Press, 1615 Oxford 1985.
[9] G. Van Tendeloo, M. Chandrasekaran, F. C. Lovey, Proc. ICOMAT-86, J I M, 868, Sendai 1987.
[10] J. Dutkiewicz, J. Pons, E. Cesari, Materials Sci Eng. **A158** 119 (1992).

REVIEWED BY: DOC. DR HAB. INŻ. BOGUSŁAW MAJOR

Received: 12 April 2000.